

615. Vibrations in stainless steel turning: multifractal and wavelet approaches

Grzegorz Litak^{a,b,1} and Rafał Rusinek^a

^aDepartment of Applied Mechanics, Lublin University of Technology,

Nadbystrzycka 36, PL-20-618 Lublin, Poland

^bDepartment of Architecture, Buildings and Structures, Polytechnic University of Marche,

Via Breccia Bianche, I-60131 Ancona, Italy

E-mail: ¹ g.litak@pollub.pl

(Received 02 November 2010; accepted 4 February 2011)

Abstract. We investigate the experimental data of the turning process and the appearance of chatter vibrations. We focused on the turning of stainless steel as the example of a special material, which belongs to a hardly machinable class. To characterize the vibration properties we used statistical, multifractal, and wavelet analyses. The multifractal approach estimates complexity of the examined time series of the cutting thrust force. We report that the evolution of the vibration towards fairly large amplitude unwanted chatter with the increasing cutting depth coincides with lowering of the complexity. The results have been confirmed by continuous wavelet analysis.

Keywords: vibrations, stainless steel, multifractal, wavelet.

Introduction and experiment

Mechanical machining processes are the main technologies to obtain designed surface [1]. Unfortunately, in certain working conditions this process is unstable to chatter vibrations which destroy the process precision and finally lower product quality [2]. These cutting instabilities are due to the complex dynamics including the memory effects of the previous tool passes, the nonuniform nature of cutting material, dry friction phenomenon between the tool and the workpiece and their contact loss [1–7]. To understand and identify the instabilities, more precise experiments using different materials were performed. In this note we analyze the time series obtained from the turning process of the stainless steel. Fig. 1a illustrates turning process geometry with specified directions.

The turning experiment has been conducted using the workpiece circular shaft of stainless steel (EZ6NCT25) with the diameter of 22 mm and the tool cutting edge angle of 45 degrees. The shaft angular velocity was fixed to about 780 rpm while the corresponding feeding ratio was 0.25 mm/rev. The sampling frequency was fixed at 2 kHz.

The measured time series of a thrust component F_y of the total cutting force are plotted in Fig. 1b. Note that vibrations in the y direction, and simultaneously oscillations of the F_y force component (Fig. 1a), influence the quality of the surface directly. Note also that the oscillations of F_y increases with the cutting depth d . Namely, starting from the case (3) we observe the considerable increase in the vibration amplitude (see cases (4) and (5) in Fig. 1b).

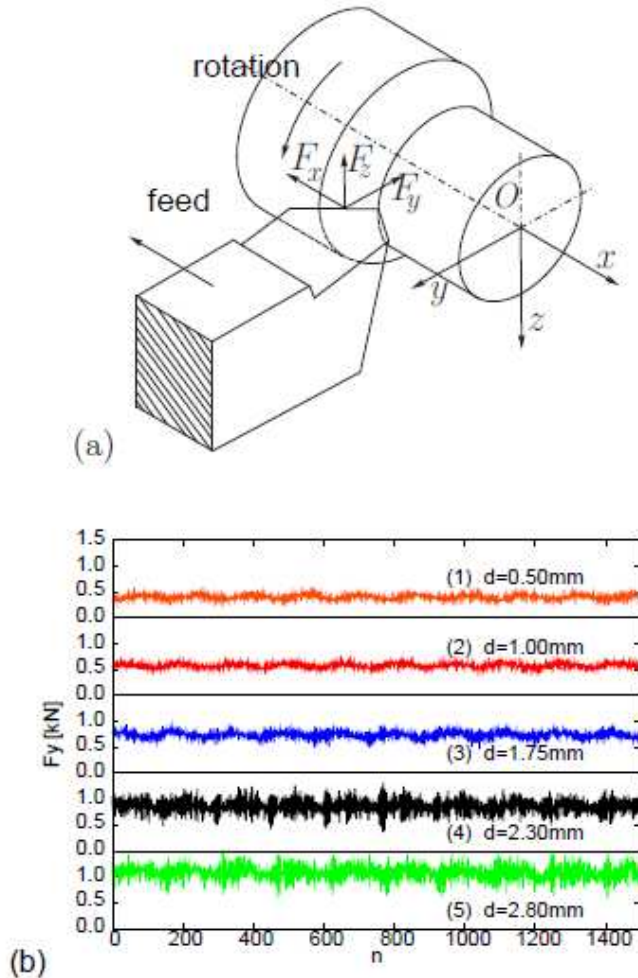


Fig. 1. (a) The schema of a turning process. The three orthogonal measured force components: feed F_x , thrust F_y , and cutting F_z . (b) F_y time series of the stainless steel turning process versus sampling number n for five different cutting depths d (referred in the text as the cases (1)–(5)). The sampling frequency was chosen at 2 kHz.

Multifractal analysis

The next step of our analysis is to estimate the critical exponent distribution estimated along the time series. In addition to a range of oscillation amplitudes, many complex processes exhibit multiple time scales. A convenient way to describe the dynamics of such multiscale processes is to use multifractals. A multifractal process evolves simultaneously over multiple time scales and requires a spectrum of scaling exponents to capture its full range of dynamics. One approach for describing such a spectrum is to use the so-called Hölder exponent. The broadness of the singularity spectrum is one measure of complexity of the process. Consider a real-valued function $F(t)$. The single Hölder exponent α of this function at a point $t_i = t_0$ is defined as follows [8,9]:

$$|F(t_i) - P_n(t_i - t_0)| \leq C|t_i - t_0|^\alpha \quad (1)$$

where $P_n(t)$ is a polynomial of degree less than α and C is a constant. For the complex systems the distribution $D(\alpha)$ form a continuous band. The property of the exponent α distributions determines the important parameters: the size of band $\Delta\alpha = \alpha_{max} - \alpha_{min}$ and the noise correlation parameter defined to the $\alpha = \alpha_{top}$ such that the distribution function $D(\alpha)$ reaches its maximum. This parameter (α_{top}), similarly to Hurst exponent, indicates how persistent the examined stochastic process is. If $\alpha_{top} < 0.5$ the process is anti-persistent (negatively correlated) while $\alpha_{top} > 0.5$ is persistent (positively correlated). The two cases $\alpha_{top} = 0.0$ and $\alpha_{top} = 0.5$ correspond to a Gaussian random process characterized by the series of random numbers and Brownian random walk characterized by random steps, respectively.

Now we apply the method of multifractals to the series presented in Fig. 1b. The resulting band is obtained by fitting the polynomial of the 8th order to the calculated points and their values for $D(\alpha) = 0$ determine α_{min} and α_{max} . In Fig. 2a we show the most interesting cases illustrating the process path to chatter (the cases (2),(3), and (4)).

Finally, in Fig. 2b we show all the cases (1)–(5) in a plane spanned by parameters $\Delta\alpha$ and α_{top} . We found that the evolution of the vibration towards fairly large amplitude vibrations with the increasing cutting depth d coincides with lowering of the complexity $\Delta\alpha$. Namely, for the sequence of the cases (2)–(5) we get $\Delta\alpha = 1.035, 0.876, 0.802,$ and $0.704,$ respectively. Furthermore, the stochastic process in chatter conditions appears to be more anti-persistent (smaller α_{top}).

More detailed information is presented in Tab. 1, where apart from the complexity results $\Delta\alpha$ and α_{top} we show the average value $\overline{F_y}$, standard deviation σ_y and kurtosis kur_y of the examined thrust force component F_y . These statistical measures simply report the increase in force with increasing cutting depth and oscillation amplitude with the similar trend but showing a fairly larger jump between the cutting depth $d = 1.75$ mm (the case 3) and 2.30 mm (the case 4).

Interestingly the kurtosis shows the non-monotonous change of the statistical distributions of F_y . Starting from the cutting depth $d = 0.50, 1.00, 2.30,$ and 2.80 mm the distribution is platykurtic - more flat than the random Gauss distribution ($kur_y = 2.815, 2.591, 2.661, 2.714 < 3,$ respectively), while for $d = 1.75$ mm we observe the leptokurtic ($kur_y > 3,$ more spiky than the Gaussian) distribution with kurtosis kur_y reaching a value of 3.40. Thus it is the largest discrepancy from the monotonic tendencies and may signal intermittency at $d = 1.75$ mm.

It should be also noted that the actual cutting depth d as well as shaft angular velocity were not constant but can be considered as the averages. In the future studies we plan to explain the role of other turning parameters on the complexity of the system response.

Table 1. Summary of the multifractal and statistical analyses

case	cutting depth d [mm]	average $\overline{F_y}$ [N]	stand. dev. σ_y [N]	kurtosis kur_y	$\Delta\alpha$	α_{top}
(1)	0.50	404.1	39.5	2.815	0.894	0.224
(2)	1.00	581.2	45.0	2.591	1.035	0.260
(3)	1.75	740.9	68.8	3.400	0.876	0.196
(4)	2.30	869.6	151.1	2.661	0.802	0.140
(5)	2.80	1084.1	158.4	2.714	0.704	0.193

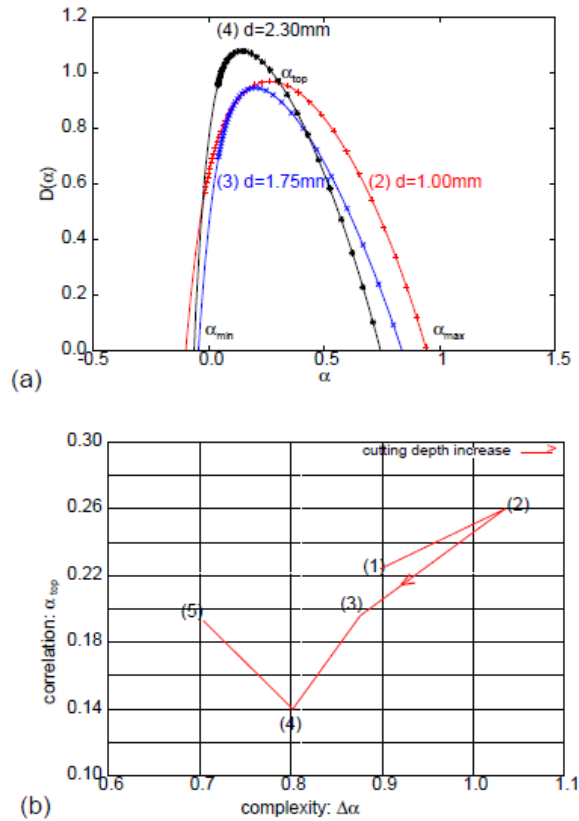


Fig. 2. (a) Multifractal bands of the three chosen cases (2)–(4) from the Fig. 1b. (b) The complexity diagram α_{top} versus $\Delta\alpha$ with all examined process denoted by numbers (1)–(5) (as in Fig. 1b).

Wavelet analysis

For the F_y time series given by $F_y(i)$, with $i = 1, 2, 3, \dots, N$, the continuous wavelet transform (CWT) with respect to a wavelet $\psi(\eta)$ is defined as follows:

$$W_{s,n}(F_y) = \sum_{i=1}^N \frac{1}{s} \psi\left(\frac{i-n}{s}\right) \frac{(F_y(i) - \overline{F_y})}{\sigma_y}, \quad (2)$$

where $\overline{F_y}$ and σ_y are the averages and standard deviations (see Tab. 1). The wavelet $\psi(\eta)$ is referred to as the mother wavelet, and the letters s and i, n denote the scale and the time indices, respectively. The wavelet power spectrum (WPS) of the F_y time series is defined as the square modulus of the CWT:

$$P_W(s, n) = |W_{s,n}|^2. \quad (3)$$

In our calculations, we have used a complex Morlet wavelet as the mother wavelet. A Morlet wavelet consists of a plane wave modulated by a Gaussian function and is described by

$$\psi(\eta) = \pi^{-1/4} e^{i\theta_0\eta} e^{-\eta^2/2}, \quad (4)$$

where θ_0 is the center frequency, also referred to as the order of the wavelet. The value of θ_0 controls the number of oscillations in the wavelet and thus controls the time/frequency resolutions. In our analysis, we used $\theta_0 = 6$. This choice provides a good balance between the time and frequency resolutions. Also, for this choice, the scale is approximately equal to the period, and therefore the terms scale and period can be interchanged for interpreting the results.

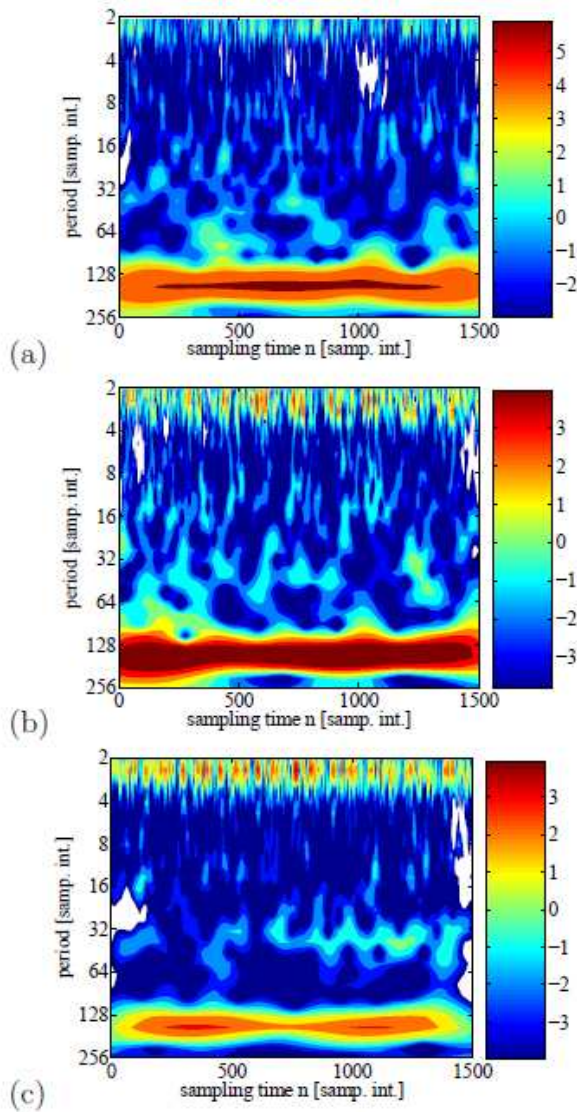


Fig. 3. Wavelet power spectra P_W for different cutting depths $d = 1.00, 1.75, 2.30$ for a, b, and c; respectively (cases (2)-(4) in Figs. 1b and 2b). The colours are related to the magnitudes of $P_W(s, n)$ according to the logarithmic scale \log_2 (see right panels marked with the corresponding scale exponents). The total measurement time of $N=1500$ samplings is related to 0.75 sec.

The reader is referred to [7,10,11] for further details on the wavelet analysis methodology.

The wavelet power spectra (WPS) of the F_y time series for the cutting depth $d = 1.00, 1.75, \text{ and } 2.30$ mm related to the chatter growing are depicted in Figs. 3a-c ($d = 1.00, 1.75, 2.30$ mm - cases (2)-(4) in Figs. 1b, 2a). Note that the slow vibration enhancement in all figures indicate the characteristic period in a vicinity of 150–160 sampling intervals which corresponds to the frequency of 12.5–13.3 Hz. This frequency is a consequence of the rotational speed of a workpiece, which was about 780 rpm. Evidently the workpiece was not ideally balanced. Furthermore, in Fig. 3a and b ($d = 1.00$ and 1.75 mm) we observe the growing role of intermittent (short time intervals) vibrations of about 32–100 sampling intervals (of about 20–62 Hz). These oscillations increase frequency range (decrease period) with increasing d (Figs. 3a-b). For $d = 2.3$ mm they form a more continuous response reaching the length 900 sampling intervals (0.45 sec.). This is a manifestation of the well-developed chatter vibrations with the frequency of about 46 Hz. Besides, growing role of very short oscillations with the period of about 2-3 sampling intervals (corresponding 0.7–1.0 kHz).

Summary and Conclusions

In summary we will note that by examining turning time series of the thrust force by different methods we not only identified chatter vibrations but followed its development. Starting from small cutting depth we observed more regular vibrations related to the rotational speed (of about 13 Hz) caused by unbalanced effects. By increasing cutting depth we found the intermittent vibrations of about 20–62 Hz, which appeared to be more continuous frequency component in the cutting depth $d = 2.30$ mm (concentrated at about 46 Hz). Note that this effect was clearly observed by wavelets.

Simultaneously, we checked that other measures like the non-monotonously growing standard deviation, and more interesting nontrivial dependences of kurtosis and multifractal parameters were sensitive to that transition. We claim that the evolution of the vibration towards fairly large amplitude unwanted chatter with the increasing cutting depth coincides with lowering of the complexity and the intermittency phenomenon with the maximum of kurtosis. Furthermore, the turning process in the chatter conditions appears to be more anti-persistent than the process in a non-chatter regime.

The appearance of chatter in the larger cutting depth implies the frictional character of vibrations [2,5,7]. However, to tell more about the material role in chatter generation we need to perform more systematic turning tests. On the other hand, the delay mechanism of chatter [1,6] can be ruled out account for visible relative decreasing of the vibration amplitude (for increasing d) related to the speed of the workpiece (about 13 Hz in Fig. 3). We are also planning to examine oscillations of 3D forces including the F_x and F_z components (Fig. 1a).

Acknowledgements

The financial support of Structural Funds in the Operational Programme - Innovative Economy (IE OP) financed from the European Regional Development Fund - Project "Modern material technologies in aerospace industry", No. POIG.01.01.02-00-015/08-00 is gratefully acknowledged. GL would like to thank prof. Stefano Lenci for hospitality during his stay in Ancona supported by the European Union Seventh Framework Programme (FP7/2007-2013), FP7 - REGPOT - 2009 - 1, under grant agreement No. 245479.

References

- [1] **Altintas Y.** *Manufacturing Automation: Metal Cutting Mechanics, Machine Tool Vibrations, and CNC Design.* (Cambridge University Press, Cambridge 2000).
- [2] **Gradisek J., Govekar E., Grabec I.** Time series analysis in metal cutting: chatter versus chatter-free cutting. *Mech. Syst. Signal. Process.* 12, 839–854 (1998).
- [3] **Gradisek J., Govekar E., Grabec I.** Using coarse-grained entropy rate to detect chatter in cutting. *J. Sound. Vibr.* 214, 941–952 (1998)
- [4] **Litak G., Rusinek R., Teter A.** Nonlinear analysis of experimental time series of a straight turning process. *Meccanica*, 39, 105–112 (2004).
- [5] **Wiercigroch M.** Chaotic vibration of a simple model of the machine tool-cutting process system. *J. Vibr. Acoust.* 119, 468–475 (1997).
- [6] **Stepan G.** Modelling nonlinear regenerative effects in metal cutting. *Philos. Trans. R. Soc. Lond.* A359, 739–757 (2001).
- [7] **Sen A. K., Litak G., Syta A.** Cutting process dynamics by nonlinear time series and wavelet analysis, *Chaos* 17, 023133 (2007).
- [8] **Goldberger A. L., Amaral L. A. N., Glass L., Hausdorff J. M., Ivanov P. Ch., Mark R. G., Mietus J. E., Moody G. B., Peng C.-K., Stanley H. E.** Physiobank, physiotoolkit, and physionet: components of a new research resource for complex physiologic signals. *Circulation* E101, 215–220 (2000) and the software on the web site <http://www.physionet.org/physiotools/multifractal/> (20 Sep. 2010).
- [9] **Litak G., Geca M., Yao B.-F., Li G.-X.** Indicated mean effective pressure oscillations in a natural gas combustion engine. *Zeitschrift fur Naturforschung* 64a, 393–398 (2009).
- [10] **Torrence C. and Compo G. P.** A practical guide to wavelet analysis, *Bull. Amer. Meteor. Soc.* 79, 61–78 (1998).
- [11] **Kumar P. and Fofoula-Georgiou E.** Wavelet analysis for geophysical applications, *Rev. Geophys.* 35, 385–412 (1997).